Structural transition in nanosized silicon clusters

D. K. Yu, R. Q. Zhang,* and S. T. Lee

Center of Super-Diamond and Advanced Films (COSDAF) and Department of Physics and Materials Science, City University of Hong Kong, Hong Kong SAR, China

The structural transition to bulk diamond structure in nanosized silicon clusters has been studied by tight-binding calculations. For intermediate-size clusters (<200 atoms), the energetically favorable structures obtained consist of small subunits like Si_{10} and Si_{12}, qualitatively consistent with the experimental fragmentation behavior of these clusters. For spherical silicon nanocrystals, the surface atoms reconstruct to minimize the number of dangling bonds, forming a continuous surface. The large curvature of the continuous surface causes lattice contraction in the nanocrystals. Present calculations predict the lattice contraction versus the particle radius as $\Delta a \approx 0.4/R$, with Δa and R in Å. By comparing cohesive energies of the two sorts of structures, the structural transition is estimated to occur in the range of 300–500 atoms, or about 2.3–2.7 nm in diameter.

I. INTRODUCTION

The study of silicon nanostructures is an active field of research because of the strong room-temperature photoluminescence (PL) and the observation of quantum size effect. Recently, the studies of silicon cluster assembled films have attracted much interest. Because the size of the deposited silicon clusters are easier to control than that of porous silicon, the study of the PL of silicon cluster films allows a more direct test of the quantum confinement model. Usually the results can be divided into two classes. For films that are composed of clusters larger than 3 nm, the PL of the silicon clusters follows the quantum confinement model very closely;[1–3] While for films whose components are smaller than 2 nm, a general failure of the confinement model based on the diamond lattice is found.[4,5] It is highly probable that the smaller clusters (<2.0 nm, 200 atoms) cannot retain a diamond structure. In fact, recent transmission electron microscopy (TEM) studies showed that no crystallized grains can be revealed for films composed of silicon grains having a mean diameter of 2 nm.[5] Goldstein also reported experimental data showing a disappearance of the crystalline contrast in the TEM images for silicon particles below 2 nm in diameter.[6] These experiments call for a reliable theoretical interpretation of the transition to a diamond structure encountered in larger silicon nanoparticles.[1,5] However, previous theoretical results have been conflicting. A combined tight-binding density-functional theory has predicted a transition at 4200 atoms, based on the geometrical and electronic structures of Si_n clusters up to $n=14$.[7] This value seems too large, probably due to the severe extrapolation from small clusters. Another work has yielded a critical size of about 50 atoms,[8] which is probably too small compared with the experimental results.

Moreover, the recent result on the fragmentation behavior of intermediate-size silicon clusters is also interesting. The intermediate-size Si_n clusters ($n<150$) fragment by fission, yielding $Si_6{}^+$–$Si_{11}{}^+$, while larger crystalline clusters evaporate Si^+ and Si_2^+ ions at higher fluence of the laser.[2] The possible explanation of this phenomenon is that the intermediate-size Si clusters are built from smaller subunits containing 6–11 atoms. While these subunits probably have quite stable cage structures they are bonded to each other rather loosely.[2]

In experiments, the nanosized silicon clusters are produced either from laser vaporization of Si wafer or laser decomposition of SiH_4. The temperature in the source zone is as high as 1200 K.[2] Then the silicon clusters are cooled down by collisions with the helium atoms during the supersonic expansion after extracting from a conic nozzle.[2] Finally, the clusters are deposited on the substrate. It has been shown that the low-energy deposition procedure (<0.5 eV/atom) will keep the structures of the clusters intact.[9] Though the Si clusters in a film might be different from the free Si clusters, we study in this paper the free Si clusters as the first step using tight-binding molecular dynamics (TBMD). The result on free Si clusters is able to give some insight to the Si cluster assembled films.

II. THEORETICAL METHOD AND COMPUTATIONAL DETAILS

The TBMD simulations we conducted for studying nanosized Si clusters might be the most suitable method for systems involving hundreds of atoms. In a tight-binding method, the Hamiltonian matrix generated in a quantum-mechanical way and the matrix equation is solved as in the case of first-principle calculations. However, the procedure of generating the tight-binding Hamiltonian is simplified by parametrizations. This makes the tight-binding method more reliable than the classical potential models but computationally more simple than first-principle approaches, applicable to large systems.

Following a transferrable tight-binding potential model proposed previously for silicon,[10] the Hamiltonian in the tight-binding model of N atoms can be written as

$$H = \sum_i \frac{P_i^2}{2m} + \sum_n \langle \Psi_n | H_{TB} | \Psi_n \rangle + E_{rep} + E_0 N. \quad (1)$$

The first term is the kinetic energy of the ions, while the second term is the band-structure energies obtained by sum-

ming up the eigenvalues of all the occupied states. The third term is a repulsive potential. E_0 is a constant energy shift to give the correct cohesive energy of the system. In the present tight-binding scheme, E_0 in the fourth term is set to be 8.74 eV.[10] The tight-binding potentials were obtained by fitting to the energies of various bulk crystal structures of Si. The radial scaling functions are similar to those employed by Goodwin, Skinner, and Pettifor,[11] but the cutoff distance is fixed for all structure configurations. This tight-binding model has been shown to be applicable in molecular dynamics and its transferability is found to be fairly good.[10]

The molecular-dynamics simulation program is written in FORTRAN, following the flow chart of TBMD scheme given in Ref. 12. The program has been tested and run on both Pentium IV personal computers and the Sun Enterprise 10000 (Starfire) system. We use the Verlet algorithm for the molecular dynamics, and choose the time step as 1.0 fs. The total-energy conservation is of the order 10^{-5} eV/atom. We use a simulated annealing method to get the energetically favorable structures of the nanosized Si clusters. Typically the clusters are equilibrated at 1200 K for several picoseconds, then cooled at a rate of 40 K/0.2 ps. For small Si_n clusters ($n \leq 20$) we have checked that the slow cooling rate can make the system reach their energetically most favorable configurations. For large clusters such as Si_{60}, it is quite difficult to find its global energy minimum either by simulated annealing or other optimization methods. It may possess a large number of local minima whose energies are close to each other. For Si_{60}, we have tested ten different cooling rates ranging from 20 K/0.02 ps to 20 K/0.3 ps. It is found that the final structures and energies are quite similar if the cooling rate is below 50 K/0.2 ps.

III. RESULTS AND DISCUSSIONS

A. Tight-binding results on small clusters

A thorough test has been performed in this work on the reliability of this tight-binding potential model in treating small silicon clusters. For very small Si_n clusters (n less than 9), it has been shown in Ref. 13 that this tight-binding potential model can yield their correct ground-state geometries. We now check if this model works in larger clusters. The two energetically favorable geometries of some small Si clusters are shown in Fig. 1. For Si_9, the lowest energy geometries are the bicapped pentagonal bipyramids, in agreement with the full-potential linear muffin-tin orbital molecular dynamics (FP-LMTO) results.[14] The total energy of Si_9 (b) is 1.14 eV lower than that of Si_9 (a), while in FP-LMTO, Si_9 (b) is 0.47 eV higher than Si_9 (a). For Si_{10}, Si_{10} (a) is a very stable structure, which has been found to be the ground-state structure in quantum Monte Carlo (MC),[15] density-functional/local-density approximation (DFT/LDA),[16] and the FP-LMTO methods.[17] Within the present tight-binding scheme, Si_{10} (a) is only 0.15 eV higher than the energetically most favorable geometry Si_{10} (b). Si_{10} (b) is a bicapped tetragonal antiprism, which was also found to be a local minimum in *ab initio* calculations.[18] For Si_{11}, we get two degenerate configurations, which can be viewed as adding one atom to Si_{10} (b). Si_{11} (a) is the energetically most favorable geometry in
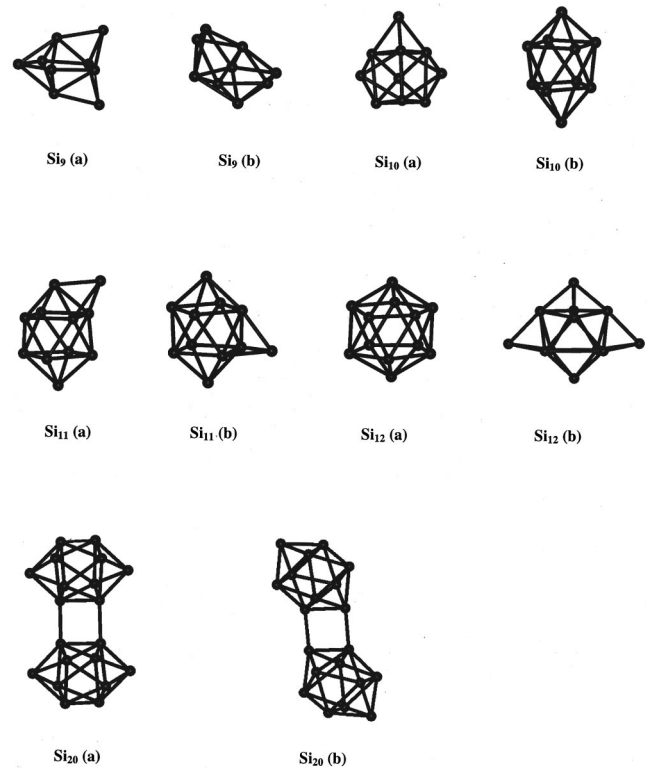

FIG. 1. The energetically favorable structures of small silicon clusters obtained from tight-binding calculations.

the DFT/LDA calculation.[16] For Si_{12}, the energetically most favorable geometry obtained is a bicapped pentagonal antiprism, Si_{12} (a). This geometry is also a candidate for the ground-state geometry of Si_{12} in the DFT/LDA calculations.[16] Si_{12} (b) is the energetically most favorable geometry found by the DFT/LDA calculations.[16] It is, however, 2.5 eV higher in energy than Si_{12} (a) within the tight-binding scheme. The energetically most favorable geometry for Si_{20} is composed of two Si_{10} subunits, in good agreement with the recent results of the quantum Monte Carlo[19] method. The only difference is that the Si_{10} subunit is Si_{10} (b), while in the MC results it is Si_{10} (a), since Si_{10} (a) is the energetically most favorable geometry in the MC method.

The above comparison of the tight-binding results with those of more accurate methods has shown that the present tight-binding scheme can give a good qualitative description of small silicon clusters. The energetically most favorable geometries from other accurate methods are also stable structures in the tight-binding scheme; the lowest energy geometries found from tight-binding calculations are at least competitive stable local minima in other methods. Therefore the tight-binding method is good enough to describe some qualitative features of the intermediate-size silicon clusters, and to study the structural transition to the bulk diamond structure.

B. Intermediate-size clusters

In order to get the energetically favorable structures of intermediate-size silicon clusters, we carry out simulated annealing studies. The starting structures are fragments of the
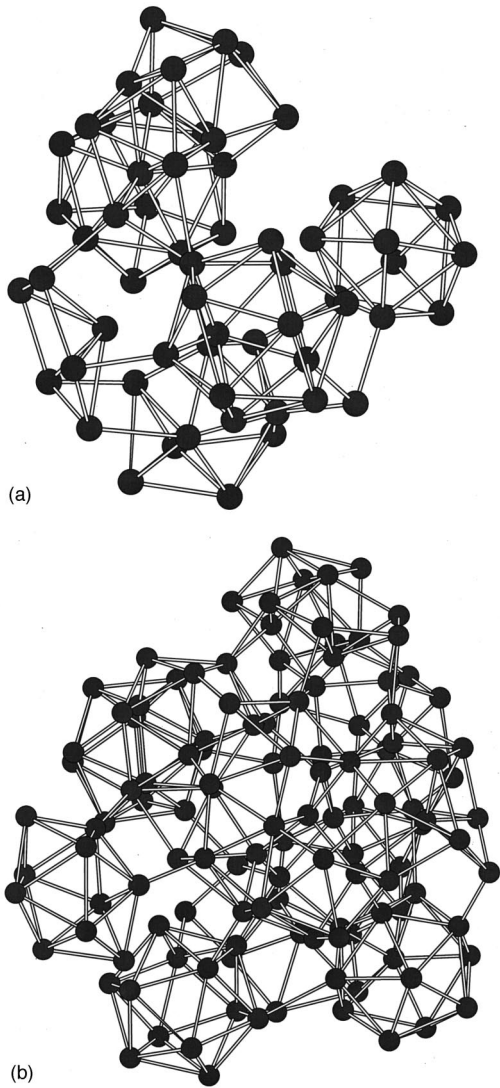
FIG. 2. Structures of Si_{60} (a) and Si_{123} (b) after annealing. All bonds below 2.8 Å are drawn out. The structures are fully relaxed, with the root-mean-square force to be 0.015 eV/Å.

bulk diamond lattice. The system is equilibrated at 1200 K for typically 4 ps (4000 steps), then cooled down at a rate of 40 K/0.2 ps. The total simulation time for one cluster is about 20 ps. Figure 2 shows two typical structures obtained from the annealing. Figure 2(a) is a 60-atom cluster, which is composed of some subunits like Si_6, Si_7, Si_{10}, and Si_{12}. These cagelike subunits are loosely connected to each other. Figure 2(b) is a 123-atom cluster. Its structure is quite similar to that of Si_{60}, except that part of the cluster is amorphous-like. The structures shown in Figs. 2(a) and (b) are qualitatively consistent with the recent experiment on the fragmentation behavior of intermediate-size Si clusters. Upon laser heating, the Si_n clusters ($n<150$) fragment by fission, yielding $Si_6^+ - Si_{11}^+$ clusters. The authors' explanation is that the Si_n clusters with $n<150$ are built from smaller subunits containing $n=6-11$ atoms.[2] While these subunits have quite stable cage structures they are bonded to each other quite loosely. This is just the case shown in Fig. 2. The annealing with lower cooling rates yields similar struc-

tures. The small cages may be rearranged, and the total energies are found to decrease a little. For example, the cohesive energy of Si_{60} with a cooling rate of 20 K/0.2 ps is about 20 meV/atom lower than that with a cooling rate of 40 K/0.2 ps, and the structure is quite similar. Since we cannot use an infinitely slow cooling rate, we can only estimate an error bar from the results of different cooling rates. The error bar for the cohesive energy is estimated to be 20 meV/atom using a cooling rate of 20 K/0.2 ps. If the clusters are kept at high temperatures ($T>1000$ K) too long, they may evaporate small cages like Si_7, Si_{10}, etc. This is consistent with the experimental fragmentation behavior.[2]

For the 191-atom ($D\sim2$ nm) and 281-atom ($D\sim2.2$ nm) particles, the annealed structures are still similar. Small cage structures appear on the surface, while the inner part is amorphous. In experiment, the smallest crystalline ordered region after long-time annealing is about 2.5 nm (~400 atoms).[20] So a 2.2-nm cluster is possibly not able to retain a diamond structure yet. The experimental annealing time for recrystallization from amorphous nanosized silicon powders is more than 1 h.[20] An MD simulation for such a long time is obviously not practical. Nevertheless, a comparison of the cohesive energies between diamond structure and the loosely connected cage structure obtained from simulated annealing as described above may allow a qualitative judgment on the energetically more favorable structure for a specific cluster.

C. Large particles

The large particles might retain diamond structure, probably with reconstructed surfaces. Atomic force microscopy (AFM) images show that the experimentally generated Si nanocrystals are spherical.[3] Accordingly, we consider here only the spherical nanoparticles. There may be a "critical" size, below which the silicon nanoparticles with diamond structure might be metastable. In order to make a direct comparison of cohesive energies between the loosely connected cage structures and the diamond structure for a smaller cluster, we need to artificially prepare diamond structures for these metastable small Si particles. To achieve them, the equilibration temperature should be selected to be high enough to allow the surface atoms to reconstruct but low enough so as not to melt the small particles in diamond structure. For such a purpose, the equilibration temperature is chosen to be 800 K, and the equilibration time to be 4.0 ps. Two cooling rates of 100 K/0.1 ps and 60 K/0.1 ps were adopted for testing, yielding similar final structures with slight difference in energy (below 5 meV/atom). Figure 3 shows the largest Si nanoparticle we obtained, corresponding to a spherical 2.5-nm particle containing 417 Si atoms. The surface is reconstructed to minimize the number of dangling bonds. The atoms on the surface tend to form a continous surface, and the step edges are considerably reduced.

In the inner part of the particle, the diamond lattice is retained. Figure 4 shows the radial distribution function of the diamond lattice core and the loosely connected cage structures of Si_{191}. For a structure with the diamond core, the nearest neighbors locate at about 2.33 Å. The second

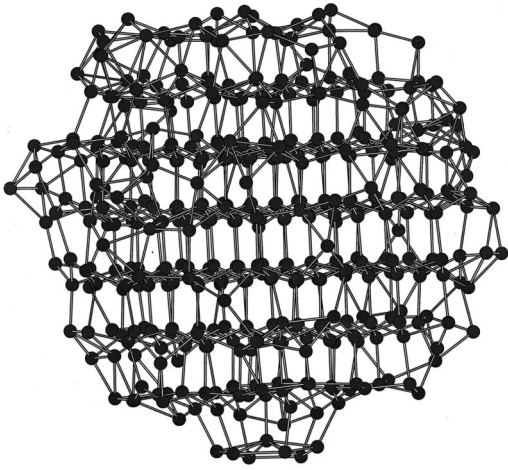FIG. 3. Structure of the 417-atom Si nanocrystal with reconstructed surface. All bonds below 2.8 Å are drawn out. The structure is fully relaxed, with the root-mean-square force to be 0.015 eV/Å.

FIG. 5. Lattice contraction versus the Si nanoparticle radius. The six circles correspond to nanocrystals containing 151, 191, 239, 281, 357, 417 atoms, respectively. The dashed line is a fitting to the data, which corresponds to $\Delta a \approx 0.4/R$.

neighbor distance has a broad distribution, indicating a lattice distortion in such small particles. The nearest-neighbor distances exhibit a small increase with increasing particle radius, and the lattice distortion decreases with increasing radius. For the loosely connected cage structures, the nearest-neighbor distance is about 2.5 Å. No positional order can be found in this structure.

It is possible that there is considerable surface tension in the region near the continuous surface due to the large curvature. Indeed, large lattice contraction is found inside the particle. Since there is some dispersion of nearest-neighbor distances, we use the average of the nearest-neighbor distances of the diamond lattice core as the lattice constant. The lattice contraction is obtained by comparing the lattice con-
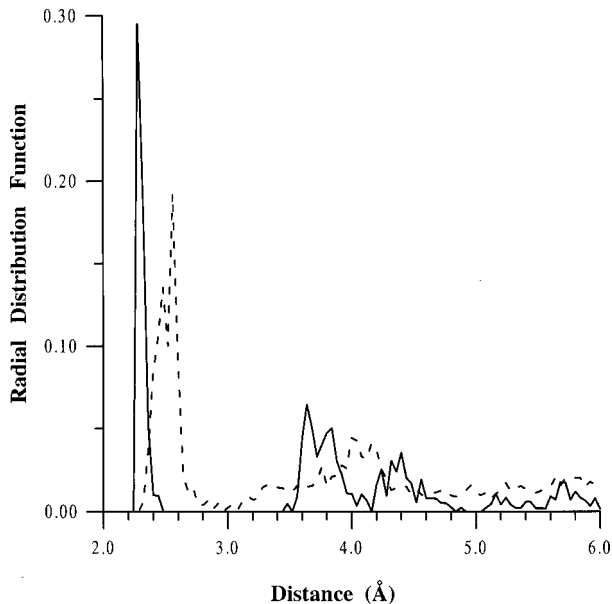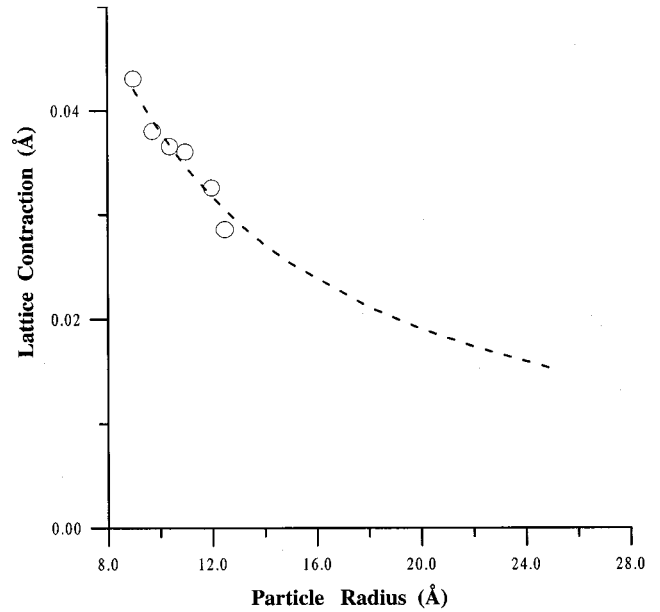
stant of the bulk (2.36 Å in the present tight-binding model) and the nanoparticle. Figure 5 shows the relationship of lattice contraction versus Si nanoparticle radius. The lattice contraction Δa decreases with increasing particle radius R. The lattice contraction is found to be roughly proportional to $1/R$ as described by

$$\Delta a \approx \frac{0.4}{R}. \qquad (2)$$

The units of Δa and R is Å. This result is obtained by fitting to only six data points. Smaller particles are unstable, while for larger particles the computational cost is too large. Nevertheless, this result is able to provide a guideline in estimating the lattice contraction in large Si nanoparticles. According to this formula, a Si nanoparticle with a diameter of 5.0 nm should have a lattice contraction of 0.016 Å. The surface reconstruction of a Si particle with an even larger R should tend to that of the bulk silicon.

In experiment, lattice contraction and dilatation have been observed in Si nanoparticles with an oxide shell.[21] The lattice strain is attributed to the Si/oxide interface. Here in pristine Si nanoparticles, the lattice strain is caused by the surface tension, which is similar to the particles with an oxide shell. We have also calculated some hydrogen saturated Si nanoparticles. In such particles, the surfaces consist of separate SiH units. These SiH units are not connected to each other to form a continuous surface. Therefore there is no surface tension. The lattice constant in the core is very close to the bulk value; surface relaxation is limited to the outermost three or four layers. This result indicates that the lattice contraction in the pristine Si nanoparticles originates from the reconstructed continuous surface.

FIG. 4. Radial distribution function of Si_{191}. The solid line is from the diamond lattice core, and the dashed line is from the connected cage structure.
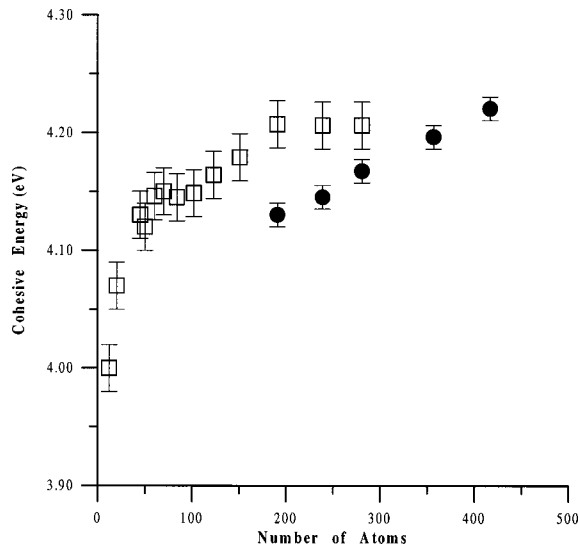
FIG. 6. Cohesive energies of the two different structures. Squares are the energies of the connected cage structures as the ones shown in Fig. 2, solid circles are energies of the spherical nanocrystals as the one shown in Fig. 3. The error bar for the connected cage structure is 0.02 eV, and 0.01 eV for the nanocrystals.

D. Structural transition in nanosized Si clusters

In determining the critical size for the structural transition, previous calculations based on a combined tight-binding and DFT/LDA method yielded a critical size of about 4200 atoms.[7] By comparing the energies of fragments of close-packed fcc crystal and diamond crystal, a linear combination of atomic orbitals (LCAO) calculation gave a critical size of 50 atoms.[8] Although a recent scanning tunneling spectroscopy measurement seems to support this result,[22] other more direct methods such as the TEM show that the critical size is above 2 nm (~200 atoms).[5]

We intend to determine the critical size by comparing cohesive energies of the two different classes of structures, namely diamond structures with reconstructed surfaces and loosely connected cage structures (shown in Figs. 2 and 3). From Fig. 6 it is shown that the cohesive energies of loosely connected cage structures seem to approach a constant for clusters larger than 200 atoms, while the cohesive energies of the diamond structure increase with increasing size. By direct extrapolation, the critical size is about 400 atoms, or a spherical Si nanocrystal of about 2.5 nm in diameter. There

are many factors that affect the accuracy of the cohesive energy, such as the effect of finite cooling rates, the accuracy of the TB method itself, etc. Using an error bar of 0.02 eV/atom for the connected cage structure and 0.01 eV/atom for the diamond structure, the structural transition is estimated to occur in the range of 300–500 atoms, or about 2.3–2.7 nm in diameter. This result is in good agreement with experiments. A recent study of the PL of Si nanocrystals as a function of the crystal size shows that the smallest nanocrystal whose PL follows the quantum confinement model is about 2.8 nm.[3] The TEM images show that the smallest crystalline region in annealed amorphous Si powders is 2.5 nm in size.[20] A failure of the quantum confinement model based on a diamond lattice in clusters smaller than 200 atoms [5] is also supportive to the present result.

IV. SUMMARY

In this paper, we have studied the structural transition to the diamond structure in nanosized silicon clusters. A tight-binding molecular dynamics combined with simulated annealing technique is employed. The tight-binding potential model for Si is quite accurate in describing the diamond structure of Si. It is also able to describe the structures and energetics of small Si clusters. After slow annealing, the energetically favorable structures obtained for intermediate-size Si_n clusters ($n < 200$) are composed of small subunits like Si_{10} and Si_{12}, qualitatively consistent with the experimental fragmentation behavior of these clusters. For spherical Si nanocrystals, the atoms on the surface reconstruct to minimize the number of dangling bonds, forming a continuous surface. The large curvature of the continuous surface causes lattice contraction in the nanocrystals. Fitting of the calculated lattice contraction versus the particle radius yields $\Delta a \approx 0.4/R$, with Δa and R in Å. By comparing cohesive energies of the two sorts of structures, the transition to diamond structure is estimated to occur in the range of 300–500 atoms, or about 2.3–2.7 nm in diameter. This result is in good agreement with recent experiments.

*Email address: aprqz@cityu.edu.hk

[1] M. Ehbrecht, B. Kohn, F. Huisken, M. A. Laguna, and V. Paillard, Phys. Rev. B **56**, 6958 (1997).

[2] M. Ehbrecht and F. Huisken, Phys. Rev. B **59**, 2975 (1999).

[3] G. Ledoux, O. Guillois, D. Porterat, C. Reynaud, F. Huisken, B. Kohn, and V. Paillard, Phys. Rev. B **62**, 15 942 (2000).

[4] P. Mélinon, P. Kéghélian, B. Prével, A. Perez, G. Guiraud, J. LeBrusq, J. Lermé, M. Pellarin, and M. Broyer, J. Chem. Phys. **107**, 10 278 (1997).

[5] P. Mélinon, P. Kéghélian, B. Prével, V. Dupuis, A. Perez, B. Champagnon, Y. Guyot, M. Pellarin, J. Lermé, M. Broyer, J. L.

Rousset, and P. Delichére, J. Chem. Phys. **108**, 4607 (1998).

[6] A. N. Goldstein, Appl. Phys. A: Mater. Sci. Process. **62**, 33 (1996).

[7] D. Tomának and M. A. Schluter, Phys. Rev. B **36**, 1208 (1987).

[8] J. R. Chelikowsky, Phys. Rev. Lett. **60**, 2669 (1988).

[9] R. Neuendorf, R. E. Palmer, and R. Smith, Chem. Phys. Lett. **333**, 304 (2001).

[10] I. Kwon, R. Biswas, C. Z. Wang, K. M. Ho, and C. M. Soukoulis, Phys. Rev. B **49**, 7242 (1994).

[11] L. Goodwin, A. J. Skinner, and D. G. Pettifor, Europhys. Lett. **9**, 701 (1989).

[12] C. Z. Wang, C. T. Chan, and K. M. Ho, Phys. Rev. B **39**, 8586 (1989).

[13] K. Zickfeld, M. E. Garcia, and K. H. Bennemann, Phys. Rev. B **59**, 13 422 (1999).

[14] B. X. Li, M. Qiu, and P. L. Cao, Phys. Lett. A **256**, 386 (1999).

[15] J. C. Grossman and L. Mitas, Phys. Rev. Lett. **74**, 1323 (1995).

[16] M. V. Ramakrishna and A. Bahel, J. Chem. Phys. **104**, 9833 (1996).

[17] B. X. Li, P. L. Cao, and M. Jiang, Phys. Status Solidi B **218**, 399 (2000).

[18] K. Raghavachari and C. M. Rohlfing, J. Chem. Phys. **89**, 2219 (1988).

[19] L. Mitas, J. C. Grossman, I. Stich, and J. Tobik, Phys. Rev. Lett. **84**, 1479 (2000).

[20] H. Hofmeister, J. Dutta, and H. Hofmann, Phys. Rev. B **54**, 2856 (1996).

[21] H. Hofmeister, F. Huisken, and B. Kohn, Eur. Phys. J. D **9**, 137 (1999).

[22] B. Marsen, M. Lonfat, P. Scheier, and K. Sattler, Phys. Rev. B **62**, 6892 (2000).